Particulate matter pollution at regional scale in Eastern France: influence of weather types and circulation regimes and sources strength during COVID-19 Lockdowns

Sarah Marion, Nadège Martiny, Suzanne Crumeyrolle, Olivier Planchon, Anaïs Detournay

Atmospheric Pollution Research 16 (2025) 102423

Contents lists available at ScienceDirect

Atmospheric Pollution Research

journal homepage: www.elsevier.com/locate/apr

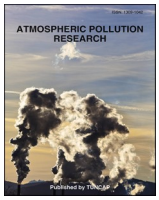

Particulate matter pollution at regional scale in Eastern France: Influence of weather types and circulation regimes and sources strength during COVID-19 Lockdowns

Sarah Marion [a,*], Nadège Martiny [a], Suzanne Crumeyrolle [b], Olivier Planchon [a], Anaïs Detournay [c]

[a] Laboratoire Biogéosciences, UMR 6282 CNRS, Université Bourgogne Europe, 6 Boulevard Gabriel, 21000, Dijon, France
[b] LOA – Laboratoire d'Optique Atmosphérique, UMR 8518 CNRS, Université de Lille, 59000, Lille, France
[c] ATMO Bourgogne Franche – Comté, 25000, Besançon, France

ARTICLE INFO

Keywords:
Air pollution
Fine particles
Ground-based measurements
Weather types
COVID-19

ABSTRACT

This study focuses on the characterization and understanding of the particulate matter pollution in two medium-sized cities located in eastern France with contrasting air quality, Dijon and Montbéliard. Measurements of PM_{10} (diameter <10 μm) and $PM_{2.5}$ (diameter <2.5 μm) concentrations are analyzed at two fixed measurement stations over the 2015–2022 period. If EU thresholds are being respected for PM_{10}, this is more difficult for $PM_{2.5}$, especially at the daily time step, and during the "particulate season" from October to April.

We then used the 8-km SAFRAN reanalyzed database and the 10-m Digital Terrain Model to analyze the climate and topography effects on air quality in the two cities. We completed this with the study of the influence of the atmospheric circulation regimes on daily PM levels variability, based on the qualitative "Groβwetterlagen".

Our study shows that the weather types may help explaining the PM levels in a city, combined with the climate-topographic effects at the urban scale. Our study also highlights, through the COVID-19 case study, the complexity of the PM pollution with respect to other pollutants like NO_x (more directly related to traffic). Finally, our study puts in stress that even in favorable air quality urban conditions, the daily $PM_{2.5}$ concentration levels exceed the recommended threshold for human health by around 8%.

1. Introduction

Over the last 20 years, concentrations of SO_2 atmospheric pollutants have decreased of 80% in France as a result of lower emissions in the industrial sectors combined with the introduction of European regulations. Concentrations of NO_2 and PM, which appear to be decreasing more slowly (−40% in the 2000–2020 period), regularly exceed EU thresholds and represent a major public health issue, specifically PM. Indeed, fine particles with a diameter below 10 μm (PM_{10}) were classified as a "definite carcinogen" by the International Agency for Research on Cancer (IARC) in 2013. In France, 40,000 premature deaths per year (or 7% of mortality) are estimated to be attributed to $PM_{2.5}$ exposure of people aged 30 (Santé Publique France, 2021) causing an increased risk of lung (Brunekreef et al., 2021; J. Chen and Hoek, 2020; Pope et al., 2002), bronchial, or tracheal cancers. In addition, two observations remain to be made: there is no PM concentration threshold below which there is no health risk (Dominici et al., 2019), and chronic exposure, even to low PM concentrations, induces significant health effects, more important than in the case of a one-off exposure to a pollution peak. For this reason, it is crucial to understand PM spatial and temporal variability and to characterize the pollution levels according to the EU thresholds and the 2021 very restrictive WHO recommendations. Moreover, what are the main explaining factors of this pollution, and at which spatial scales? Circulation regime is, for instance, a significant factor to be taken into account at the synoptic scale (Giovannini et al., 2020), particularly in terms of their potential influence on the concentration levels measured and the accumulation-dispersion phenomenon. For example, a prolonged anticyclone can lead to air stagnation, favoring the accumulation of pollutants when heavy frosts occur in winter (Planchon et al., 2009, 2015; Quénol et al., 2008) and heatwaves in

* Corresponding author.
E-mail addresses: sarah.marion@u-bourgogne.fr (S. Marion), nadege.martiny@u-bourgogne.fr (N. Martiny), suzanne.crumeyrolle@univ-lille.fr (S. Crumeyrolle), olivier.planchon@u-bourgogne.fr (O. Planchon), anais.detournay@atmo-bfc.org (A. Detournay).

https://doi.org/10.1016/j.apr.2025.102423
Received 13 November 2024; Received in revised form 16 January 2025; Accepted 16 January 2025
Available online 18 January 2025

summer (Lupo et al., 1997; Mokhov et al., 2014), while a westerly or northerly flow could disperse these particles. What about the micro-scale determinants, notably the urban climate around the measurement station? The urban environment plays a crucial role in the spatial distribution of air pollution, particularly at the local scale. Dupont et al. (2016) highlight the crucial role of boundary layer dynamics in modulating fine particulate matter concentrations during extreme air pollution events in urban environments. Similarly, Arkouli et al. (2010) found that PM concentrations were highest during land wind events, highlighting the importance of local meteorological conditions in shaping air quality.

In France, the AASQA (Association Agréée de Surveillance de la Qualité de l'Air - Approved Air Quality Monitoring Association) constitute the national air quality structure whose missions are to measure and monitor air quality in each French region with the technical and scientific support of the LCSQA (Laboratoire Central de Surveillance de la Qualité de l'Air - Central Air Quality Monitoring Laboratory), which is tasked by the State to provide the reliability of outdoor ambient air measurements in accordance with European directives. More than 720 fixed measurement stations have been installed throughout France, managed by ATMO, the regional air quality monitoring network. This study focuses on the air quality in Bourgogne Franche – Comté (BFC), a region located in eastern France, with a relatively dense network of 21 p.m. measurement stations. Moreover, we estimate that 27% of the BFC population is "chronically" exposed to $PM_{2.5}$ (Loones et al., 2021), which means exposed to $PM_{2.5}$ concentrations above the 10 $\mu g/m^3$ annual WHO recommendation threshold over 3–4 years during the period from 1 January 2016 to 31 December 2019. In BFC, we choose to zoom on two cities: Dijon Metropolis and Pays de Montbéliard (PMA), representative of medium-sized European cities (respectively 159,106 and 25,726 inhabitants) with a clear gradient in air quality conditions. Over the 2015–2022 period, relatively low annual levels of $PM_{2.5}$ (9.02 $\mu g/m^3$) and PM_{10} (15.95 $\mu g/m^3$) were observed in Dijon linked to agricultural influence in spring. In Montbéliard, where large automotive industries are implanted, mean annual $PM_{2.5}$ and PM_{10} concentrations are measured at 10.96 $\mu g/m^3$ and 17.44 $\mu g/m^3$, respectively. These values are below the $PM_{2.5}$ EU annual threshold of 25 $\mu g/m^3$ applied by the AASQA at both sites. However, at the urban level, 78.9% of the population of the Pays de Montbéliard (PMA) was regularly exposed on 1 January 2018, compared with only 7.7% of the population of Dijon Métropolis. Analyzing reference data over an extended period allows for a more comprehensive assessment of air quality by accounting for variations in pollutant concentrations between geographically proximate cities, which may experience distinct influencing factors in terms of particulate matter exposure. Beyond this, the aim of this work is to propose a method of analysis that can be applied to comparable cities in order to refine existing knowledge on urban air quality.

The specific objective of this study is twofold. First, we aim at characterizing particulate pollution (PM_{10} and $PM_{2.5}$) and its spatio-temporal variability at a regional scale in eastern France, focusing on two medium-sized cities representative of the European context, Dijon and Montbéliard (§3.1.1), with a good air quality index but experiencing contrasted particulate matter pollution, with a significant health issue related to the $PM_{2.5}$ fraction (§3.2.2 and §3.3). Second, we aim at delimiting how and to what extent the particulate pollution is influenced by large scale factors such as climate and topography conditions that impact the PM levels at a daily time-step during the "particulate season" in eastern France. We adopt here the original approach of weather type (§3.2.1 with the 8-km SAFRAN grids and §3.2.2 with the qualitative "Groβwetterlagen") in order to explain more precisely the air quality in BFC when existing literature mainly analyzes the relationship between air quality and each climate variable separately. Lastly, we seized the opportunity of studying the changes in traffic during the COVID-19 lockdowns on $PM_{2.5}$ pollution in both cities (§3.3).

2. Materials & methods

For this work we used PM_{10} and $PM_{2.5}$ data from ATMO, measured at an hourly time step, in order to carry out an air quality diagnosis of the region of interest, focusing on Dijon and Montbéliard cities and their specific features.

2.1. Studied area

The Bourgogne Franche – Comté (BFC) region, located in eastern France, has three major mountain massifs, with relatively low altitudes (average altitude ranging from 500 to 800 m). In the east, the Vosges and Jura massifs meet in the Belfort Gap, while the Morvan dominates the west (Fig. 1). The region has a temperate oceanic climate (*Cfb* in the Köppen Geiger classification (Köppen, 1936)). This climate is defined by mild, wet winters (average temperatures in the 3 coldest months range from 0 °C to 18 °C) and cooler summers (average temperatures between 12 °C and 25 °C, with heat waves attenuated by the dominant winds).

The 21 ATMO PM measurement stations in the BFC region are distributed as follows: 12 stations measure the PM_{10} granulometric fraction (circles in Fig. 1) and only 9, the $PM_{2.5}$ concentrations levels (diamond-shaped in Fig. 1). This is partly explained by the later EU regulation of the finest particles (in 2009). Furthermore, if we consider the concentration levels, it can be observed that the average annual PM_{10} concentrations over the historical air quality period (2015–2022) are generally in line with or close to the annual WHO threshold of 15 $\mu g/m^3$, while $PM_{2.5}$, for which the annual WHO recommendations is 5 $\mu g/m^3$, are exceeded at all stations, including the rural Morvan site (approximately 7 $\mu g/m^3$).

In 2022, the BFC region was evenly impacted by a high level of PM_{10}, with agriculture and the residential sector being the main emission sectors (29% each), never exceeding the European annual threshold of 40 $\mu g/m^3$ while the WHO annual threshold (15 $\mu g/m^3$) was approached or even exceeded over most of the region. As for $PM_{2.5}$, there are slight disparities between rural areas (recording the lowest levels) and urban areas (recording the highest levels), exposed in particular to traffic and exceeding the WHO threshold (5 $\mu g/m^3$) as opposed to the European threshold (20 $\mu g/m^3$).

Among these stations, the Dijon (annotated "PEJ" for Péjoces) and Montbéliard (annotated "LEV" for Lévy) stations are located in the central-eastern part of the region. Montbéliard is a key city with its environment and topography, developed in the Belfort Gap, close to the Jura mountains, whereas Dijon is mainly on the plain, bordered by a plateau to the west (Fig. 1).

The thermic atmosphere characterized by the Local Climate Zones (Fig. 2) also highlight specific features (§2.3.4) of these two cities. Dijon is a highly residential area, with building density and height decreasing from the center to the urban surroundings, replaced by agricultural land (non-irrigated arable land to the east against a mix of mixed forests, complex cropping patterns pastures and arable land to the west). There are also large commercial areas and few town parks. PEJ station is located in the south-east of Dijon (Fig. 2a) in a generally open environment, close to large planted residential areas and to agricultural plains. The main PM sources in Dijon PEJ are residential in winter and agricultural during spreading in spring. In Montbéliard, the city is concentrated at the bottom of a valley and built around a main road, limited by the topography where the more natural areas can be found. There is a large proportion of residential housing, but also a large industrial complex (Stellantis) of 202 ha across Montbéliard (in grey, Fig. 2b) and the neighboring town, Sochaux. The LEV station is located in the city center (Fig. 2b) in a predominantly built-up environment close to the road (>3 m), constituting the majority of the municipal area. The main PM sources in Montbéliard LEV are residential in winter and intermediate traffic.

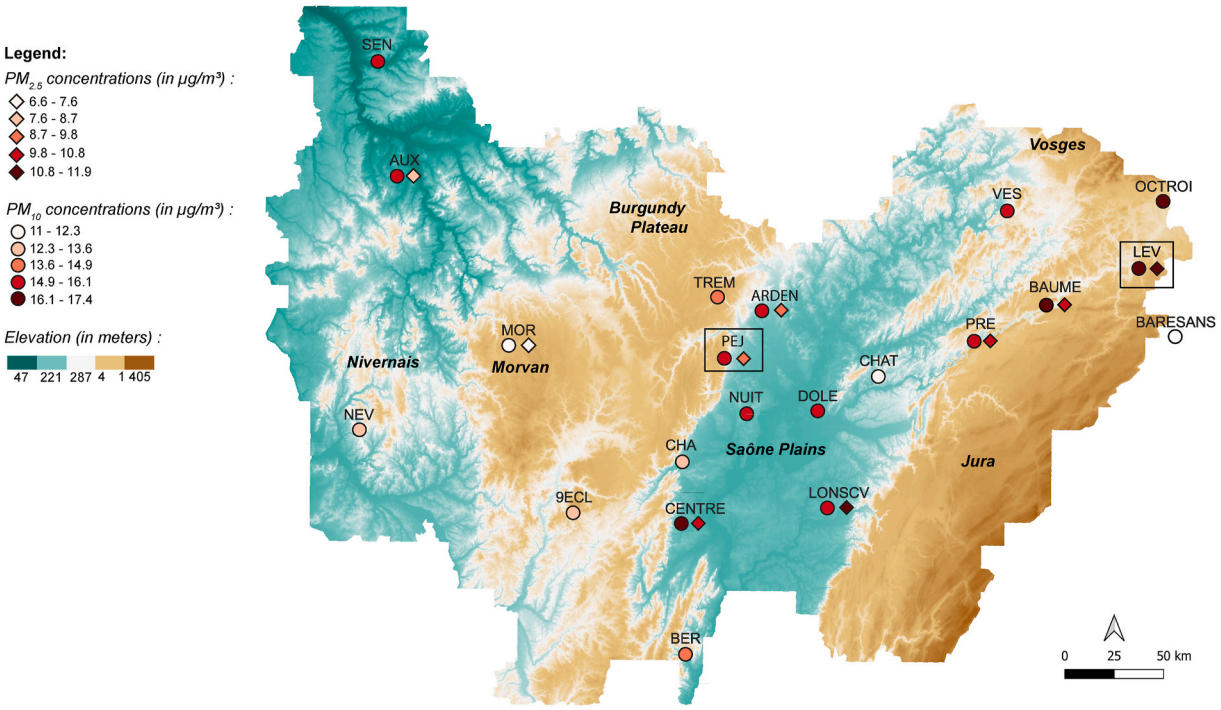

Fig. 1. Map of PM_{10} and $PM_{2.5}$ measurement stations in the BFC region. Average concentrations over the 2015–2022 period and topography (elevation in meters) are presented. Study sites are bordered in black: PEJ for "Péjoces" PM measurement station in Dijon, and LEV for the "Lévy" PM measurement station in Montbéliard.

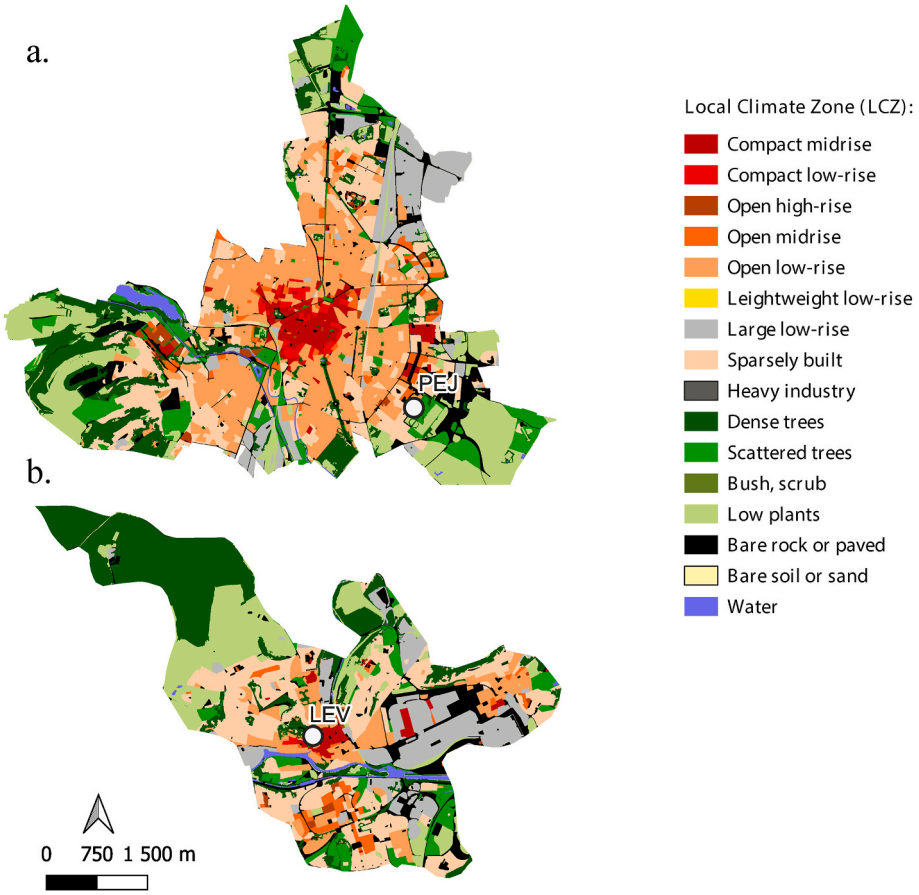

Fig. 2. Local Climate Zones (LCZ; adapted from GeoClimate (Bocher et al., 2021), see §2.3.4) in Dijon (a.) and Montbéliard (b.). Repositioning of study stations: PEJ in Dijon and LEV in Montbéliard.

2.2. Instrumentation in Dijon and Montbéliard

In Dijon, the Péjoces station (PEJ) is a peri-urban station, while in Montbéliard, the Lévy station (LEV) is an urban station. A peri-urban station is located on the outskirt of the conurbation and is considered to be representative of maximum exposure linked to secondary pollution. An urban station is located in towns and cities outside the immediate influence of traffic or industry, this equipment is considered to be representative of the air breathed by the majority of the city's inhabitants. Despite these AASQA's characterization, stations are supposed to be representative of air quality at the city level because ATMO differentiates the geographical classification of the stations and their air quality typology. Montbéliard – Lévy and Dijon – Péjoces are both considered to be background or "unexposed" stations, compared with traffic or industry other stations.

Both ATMO stations are based on the measurement principle offered by the Beta Attenuation Monitoring, or BAM, which is currently the most reliable and accurate for measuring particulate matter concentrations (Shukla and Aggarwal, 2022). The BAM is a particle analyzer (in this case, PM_{10} and $PM_{2.5}$) sampling aerosols on a filter belt before measuring mass using beta rays (frequency = 1 h). The particles arrive at the sampling head and stick to a filter belt that passes in front of a beta ray analyzer. The commonly accepted uncertainty for BAM measurements is $\pm$ 5 µg/m^3 (Met One Instruments, 2024).

2.3. Data and methods

2.3.1. Ground-based PM measurements: station data and pre-processing

The *in situ* data used are PM_{10} and $PM_{2.5}$ concentrations levels at an hourly time step from 1 January 2015 to 31 December 2022, aggregated to a daily time step according to the European and WHO time step for particulate pollution thresholds application.

PM concentrations below 0 (between −5 and 0 µg/m^3) were retained, the device's uncertainty being $\pm$ 5 µg/m^3. In order to create a homogeneous database and avoid values considered to be "extreme", PM concentrations were pre-processed over the entire series in accordance with the method used by the AASQA, on an hourly time step, as follows:

$$PM[i+1] > PM[i]*3 = NA \quad (1)$$

Where i represents the i-th concentration at an hour h and NA means the removal of the (i-th concentration +1 h).

2.3.2. Modelized meteorological data: SAFRAN grid, clustering method

SAFRAN is a mesoscale analysis system for near-surface atmospheric variables (Le Moigne et al., 2020; Soubeyroux et al., 2008). It uses surface observations combined with analysis data from meteorological models. The parameters (temperature, humidity, wind, solid and liquid precipitation, incident solar and infrared radiation) are analyzed at a 300-m altitude steps. They are then interpolated on a regular calculation grid (8 × 8 km). SAFRAN grids are available for the 1960–2022 period at a daily time step for the whole French territory.

We use the SAFRAN grids for the 2015–2022 period, in order to align with the air quality data sets (see §2.3.1).

We analyzed 4 meteorological variables (temperature, relative humidity, wind, liquid precipitation) with a daily time step, for all years and then, averaged over the 8 years. The study of the mean seasonal cycle of PM is another key input, so that the "particulate season" has been defined (day of year 1–100 and 275–365) and chosen as the target period for fine particle pollution study.

The k-means method (non-hierarchical), was used to identify meteorological clusters across the BFC region. The algorithm objective is to classify points into k homogeneous and compact groups. To determine the cluster number, the Elbow method is applied, based on the notion of "inertia". This is the sum of the Euclidean distances between each point and its associated centroid.

2.3.3. Groβwetterlagen: circulation regimes catalogue

The analysis of PM spatio-temporal variability must take into account the variety of disturbance trajectories available using the Hess-Brezowsky classification of circulation patterns (Hess and Brezowsky, 1952). The Hess-Brezowsky method is based on the pressure field at sea level and at an altitude of around 5000 m (geopotential at 500 hPa) over the North Atlantic Ocean and Europe. The classification distinguishes 29 types of circulation, known as "Großwetterlagen" (GWL). The daily catalogue of GWLs is archived and available on the Deutscher Wetterdienst website (http://www.dwd.de/GWL) and used in various studies assessing frequency trends, changes in the duration of events and transition probabilities between GWL types (Bárdossy and Caspary, 1990; Klaus, 1993). Weather types, taking into account air flows and pressure systems (high pressure or low pressure), also play a crucial role in the dispersion or accumulation of particulate pollution in the atmosphere. Analysis of Groβwetterlagen is therefore useful not only for medium-term climate forecasts, but also for understanding particulate pollution episodes and their seasonal variability.

The study of weather types (Cantat and Savouret, 2014) enables us to highlight the inter-annual specificities in terms of atmospheric circulation, in particular through the comparative study of two years considered to be meteorologically similar, 2018 and 2020 (Météo France, 2021), due in large part to these two years being the hottest since 1900. For the COVID-19 study, each day of the two years was classified as either high-pressure or low-pressure.

2.3.4. Urban thermal atmosphere: Local Climate Zones

Local Climate Zones (LCZ) are a standardized classification of urban and rural environments (Stewart and Oke, 2012) based on the physical characteristics of the landscape, such as vegetation cover, building density and urban morphology. LCZ can be used to spatialize urban environments for a better fine-scale (intra-urban) approach and to quantify the impact of urbanization on local climate. This is a classification based on analysis of surface features into 10 classes (4 naturals and 6 urbans or anthropogenic). Here, the LCZ are more precise by implementing an algorithm in the GeoClimate software in order to identify the LCZ based on vector data such as: building footprint, transport networks, water and vegetation, etc. (Bernard et al., 2024). LCZ are presented for Dijon and Montbéliard in Fig. 2.

3. Results and discussion

First, it is important to establish a diagnosis of the air quality at the two study sites (3.1) before approaching atmospheric conditions as a factor influencing fine particles concentrations (3.2). This work will be completed by the preliminary results of a study carried out on COVID-19 lockdowns in 2020 (3.3).

3.1. Diagnostic of the particulate pollution in Dijon and Montbéliard from 2015 to 2022

PM, which is a multi-sources pollutant, involves a multi-temporal analysis to better diagnose the air pollution on an annual basis (3.1.1), over the particle season (3.1.2) and, on a finer scale, over the day (3.1.3).

3.1.1. Mean annual levels of PM_{10} and $PM_{2.5}$ concentrations (2015–2022)

For the 2015–2022 period, the mean annual level of PM concentrations (Table 1) in both cities (PM_{10}: PEJ = 15.95 µg/m^3, LEV = 17.44 µg/m^3; $PM_{2.5}$: PEJ = 9.02 µg/m^3, LEV = 10.93 µg/m^3) are below the EU annual thresholds (40 µg/m^3 for PM_{10} and 10 µg/m^3 for $PM_{2.5}$). The annual PM_{10} quality target of WHO is respected in both cities based on 2005 WHO recommended value (i.e. 20 µg/m^3 for PM_{10}). This is also the case for the $PM_{2.5}$ pollutant (10 µg/m^3), but to a lesser extent, and especially in Montbéliard. However, considering the 2021 WHO recommendations, neither the PM_{10} nor the $PM_{2.5}$ mean annual

Table 1
Annual averaged concentrations from 2015 to 2022 for PM_{10} and $PM_{2.5}$ fractions in Dijon (grey area) and Montbéliard (white area). Highlighting 2021WHO threshold daily exceedances (in %) for year and PM season period. Bold numbers highlight the year when each site comply to the 2005 WHO thresholds.

	Years	2015-2022	2015	2016	2017	2018	2019	2020	2021	2022
PM10	PEJ	15.95	/	/	13.66	17.45	16.37	15.94	15.76	16.46
	LEV	17.44	20.71	18.53	19.60	19.62	16.66	14.82	13.94	15.47
PM2.5	PEJ	9.02	13.48	11.87	10.09	**8.15**	**6.83**	**6.89**	**7.55**	**7.40**
	PEJ out/year (%)	/	28.33	24.40	14.97	11.93	8.81	6.14	9.21	8.58
	PEJ out/PM season (%)	/	24.44	20.86	13.85	11.33	7.98	6.14	9.14	8.31
	LEV	10.96	13.62	13.42	10.73	11.17	10.65	**9.67**	**9.49**	**8.88**
	LEV out/year (%)	/	31.37	30.36	20	22.77	19.55	16.99	19.55	18.83
	LEV out/PM season (%)	/	29.58	27.82	19.45	22.5	17.35	16.99	17.90	18.28

concentrations meet the quality target (15 $\mu g/m^3$ for PM_{10} and 5 $\mu g/m^3$ for $PM_{2.5}$).

Since 2015, annual PM_{10} concentration levels are stable for Dijon and highlight a decrease in Montbéliard (from 20.71 $\mu g/m^3$ in 2015 to 15.47 $\mu g/m^3$ in 2022). It should be noted that the measuring equipment was replaced in 2018 at both sites, leading to an insignificant reduction in concentration levels. For $PM_{2.5}$, there has been a decrease over the last 8 years, even if the phenomenon, common to both sites, seems to be "slower" in Montbéliard (Table 1). If both sites comply with the 2005 WHO annual threshold, Dijon respects this quality limit since 2018 (8.15 $\mu g/m^3$), whereas Montbéliard had to wait until 2020 (9.67 $\mu g/m^3$). As a result, the 2021 stricter WHO quality objective (5 $\mu g/m^3$) has not been respected either in Dijon, nor in Montbéliard, this being more pronounced for $PM_{2.5}$ pollutant. Annual averages of $PM_{2.5}$ are +5 $\mu g/m^3$, to the WHO threshold which means that people are chronically exposed to the finest regulated particulate matter pollution, whatever the city considered (Health Effects Institute & Institute for Health Metrics, 2020).

We will now diagnose if there is a period of the year which favors this chronicle exposition.

3.1.2. A marked PM seasonal cycle

As expected, the PM mean seasonal cycle in Dijon and Montbéliard show a similar marked seasonal pattern, with a maximum in January and a minimum in July (Fig. 3). At the daily time step, the PM concentrations, for each size fraction, are always higher in Montbéliard than in Dijon, whatever the day considered, with the hierarchy between particle size fractions always respected at both sites ($PM_{10} > PM_{2.5}$). This observation is in line with existing literature (Cesari et al., 2018; Z. Chen et al., 2018; J. Zhang et al., 2024) emphasizing the role of residential heating-related emissions during the colder months in eastern France (see §3.2.1 for the climate analysis).

In Montbéliard, this effect may be slightly higher than in Dijon as there is more traffic and the heating network is less centralized thus

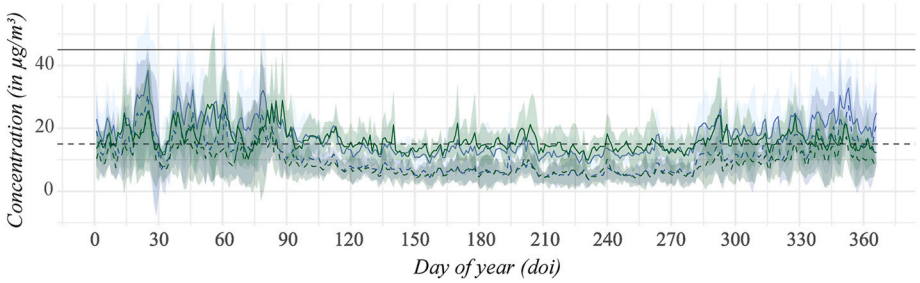

Fig. 3. Daily PM_{10} (in colored solid line) and $PM_{2.5}$ (in colored dotted line) concentrations in Dijon (in green) and Montbéliard (in blue) over the 2015–2022 period. The 2021 WHO daily recommendations value (PM_{10} in solid black line, $PM_{2.5}$ in dotted black line).

likely to be less efficient. For PM_{10}, concentrations measured in January in Montbéliard are close to 38 μg/m^3 and around 25 μg/m^3 in Dijon, so that both sites comply with the 2021 WHO daily threshold of 45 μg/m^3. For $PM_{2.5}$, Montbéliard has, on average, 22% of days exceeding a concentration of 15 μg/m^3 over the 8 years considered while Dijon has 15%. As a result, the "particulate season" is determined by the quantification of exceedances of the WHO 2021 daily $PM_{2.5}$ threshold for each year from 2015 to 2022 and corresponds to the periods during which 90% of exceeding values are observed. The pronounced "particulate season" observed in Dijon and Montbéliard spans from 1 January to 10 April and from 3 October to 31 December, i.e. from day 1 to day 100 then from day 275 to day 365.

Surprisingly, the key difference between the two cities emerges outside the "particulate season," where the concentrations in Dijon drop sharply, while those in Montbéliard remain relatively stable. This pattern underscores the strong link between air quality, local climate conditions, and topography (§3.2.1 for detailed analysis). While Dijon benefits from a milder climate and better atmospheric dispersion due to its more favorable topography (less prone to stagnation of pollutants), Montbéliard's elevated concentrations are sustained even during off-season periods. This reflects the combined influence of more localized pollution sources and geographical features, such as valley locations, which trap pollutants and exacerbate their persistence in the air. The findings corroborate the established relationship between topography and pollutant behavior, as noted in broader studies on air quality and urban geography (B. Cheng et al., 2024; Samek et al., 2020; L. Zhang et al., 2020).

As a summary, the PM pronounced seasonal cycle in eastern France is due to the residential heating-related emissions during the colder months in eastern France, thus directly to regional climate conditions (see §3.2.1 for the demonstration). In particular, this is quite interesting to note the $PM_{2.5}$ levels in summer in Montbéliard, which means that people are chronically exposed to levels close to WHO threshold in a particular topographical configuration, all year round. For this reason, and considering that the PM_{10} daily concentrations is close to the 2021 WHO strict recommendations, the rest of this work will focus on the finest fraction and during the particulate season, as this is period during which the $PM_{2.5}$ concentrations mainly exceed the threshold of 15 μg/m^3.

3.1.3. *The $PM_{2.5}$ during the particulate season*

From a public health perspective, chronic exposure to $PM_{2.5}$ is a major concern, particularly regarding exceedances of the World Health Organization (WHO) recommended thresholds. This paragraph aims to analyze daily $PM_{2.5}$ concentrations during periods when these thresholds are exceeded. Density distribution of the daily $PM_{2.5}$ concentrations above the WHO recommendation (15 μg/m^3) over the particulate seasons from 2015 to 2022 are plotted for Dijon and Montbéliard (Fig. 4).

This approach, both spatially and temporally fine-scaled, allows us to highlight specific variations in concentrations and investigate pollution sources in greater detail during particulate season. The results of our analysis show that, in general, Montbéliard consistently presents higher levels of "exceeding" $PM_{2.5}$ concentration compared to Dijon, as confirmed by the concentration densities illustrated in Fig. 4. In 2021 and 2022, Montbéliard shows a maximum concentration density approximately half that of Dijon (0.100 vs. 0.200), although this maximum is similar in other years. In Dijon, the density function remains relatively stable over time, with a peak at 18 μg/m^3. For higher value classes, the density is approximately 0.025 at 30 μg/m^3, 0.010 at 40 μg/m^3, and almost zero above 50 μg/m^3. In contrast, in Montbéliard, the density function shifts slightly towards 20 μg/m^3, and the modes are flatter at low values. For the other $PM_{2.5}$ concentration classes, the density is 0.030 at 30 μg/m^3, 0.015 at 40 μg/m^3, and 0.005 above 50 μg/m^3. While the range of high values remains comparable, it remains higher in Montbéliard. 2021 (light blue lines in Figs. 4) and 2022 (dark blue lines in Fig. 4) show a peak in $PM_{2.5}$ concentrations that slides towards higher values in the post-COVID-19 period, raising questions about the impact of sources present on site. Indeed, at the maximum of the distribution the concentrations are +5 μg/m^3 above the WHO recommendation, whereas in Dijon the levels have been +3 μg/m^3 for several years. This pattern underscores the importance of local factors, such as residential heating and traffic, as well as the impact of topography on the accumulation phenomenon of particulate matter.

To further refine these observations and better understand the $PM_{2.5}$ concentration variations, it is essential to consider the diurnal cycle, which adds another layer of insight into local behaviors such as traffic.

The analysis of diurnal cycles (Fig. 5) reveals specific features for each station, particularly in Montbéliard, where concentrations peak consistently between 6 and 9 a.m. and again after 7 p.m., mainly related to morning and evening commuting. This pattern is more nuanced in Dijon, where diurnal peaks are less pronounced (max 15 μg/m^3 in the mornings and min 9 μg/m^3 at night) and limited to a few days. This is related to the nature of the measurement station which is more influenced by residential effects than traffic (see §2.1). During commuting periods, Montbéliard records a higher daily gradient in $PM_{2.5}$ concentrations than Dijon (max 13 μg/m^3 in the mornings and min 12 μg/m^3 at night), highlighting the strong link between traffic and pollution on the site. These finer-scale results help explain the density functions observed in Montbéliard, which are heavily influenced by road traffic, and also raise questions about the influence of atmospheric conditions at the microscale, such as accumulation phenomena (Badach et al., 2023; Chan et al., 2000). This will be addressed further in section 3.2.2.

As a summary, the detailed analysis of air quality in Dijon and

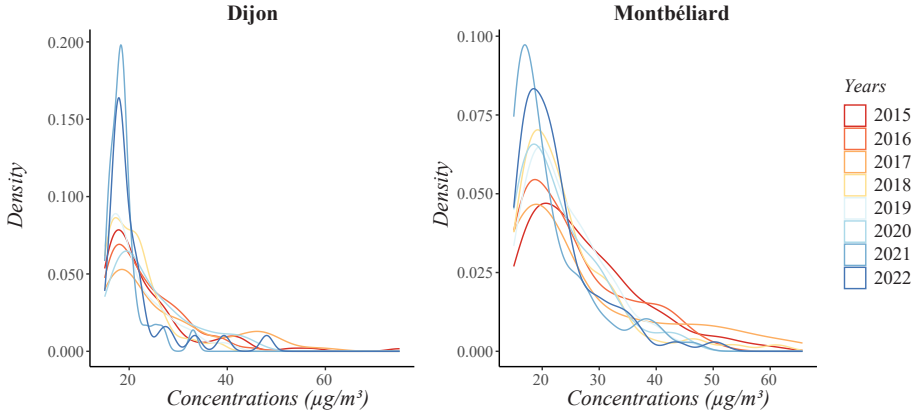

Fig. 4. Density of average daily concentrations above the WHO recommendation of 15 μg/m^3 measured over the 2015–2022 period during the particulate season (day of year 1–100 and 275–365) in Dijon and Montbéliard.

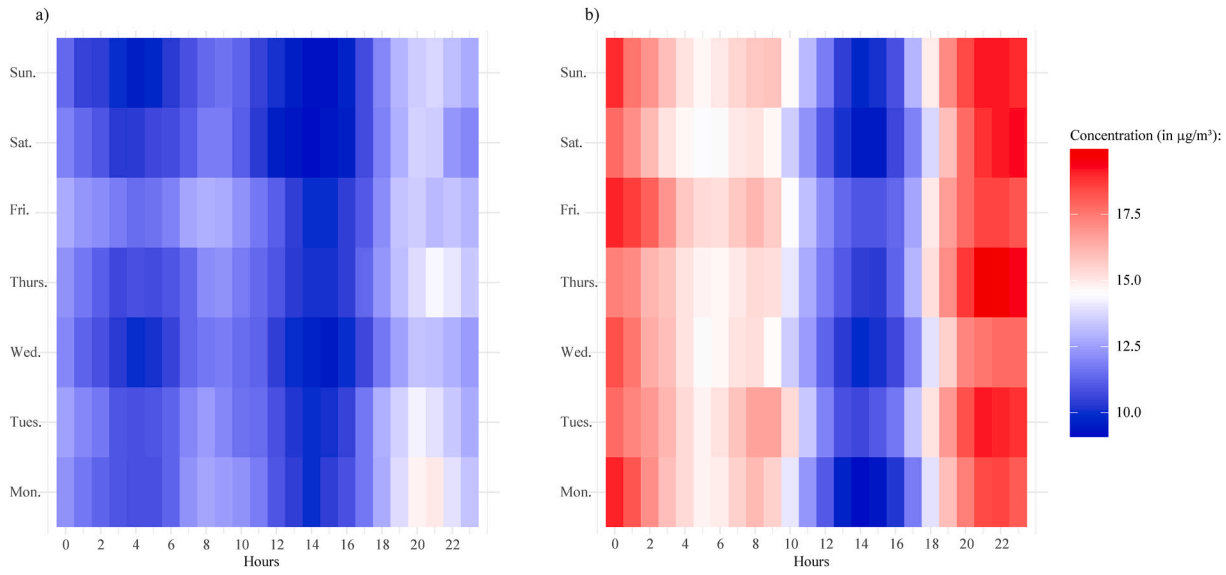

Fig. 5. Mean diurnal cycle of $PM_{2.5}$ in Dijon (a) and Montbéliard (b) depending on the day of the week (Monday to Sunday). The period considered is the 2015–2022 period.

Montbéliard, and specifically the analysis of $PM_{2.5}$ diurnal cycles, clearly shows that the differences in $PM_{2.5}$ concentrations in both cities are largely linked to local factors such as traffic, combined with large-scale topography. These elements are crucial for refining our understanding of pollution sources and improving air quality management at a microscale level. The next part of the work aims at analyzing the climate conditions that impact the PM levels at a daily time-step during the "particulate season" in eastern France. We adopt here the original approach of weather type (§3.2.1 with SAFRAN and §3.2.2 with the GWL) in order to explain more precisely the air quality in BFC when existing literature mainly analyzes the relationship between air quality and each climate variable, separately. Lastly, we seized the opportunity of studying the changes in traffic during the COVID-19 lockdowns on $PM_{2.5}$ pollution in both cities (§3.2.3).

3.2. *Influence of the atmospheric conditions on air quality*

3.2.1. *Climate in the particulate season: cluster analysis*

Atmospheric modulators of air quality are here studied by clustering the BFC region (Fig. 6). This method enables us to demonstrate the impact of climate on the PM seasonal cycle in Dijon and Montbéliard (Fig. 3) and more specific characterics during the particulate season. Meteorological factors like average temperature, relative humidity, wind, and liquid precipitations (Z. Chen et al., 2018; Kukkonen et al., 2005) have made it possible to determine 3 major "weather types" corresponding to a specific area referred to as "clusters".

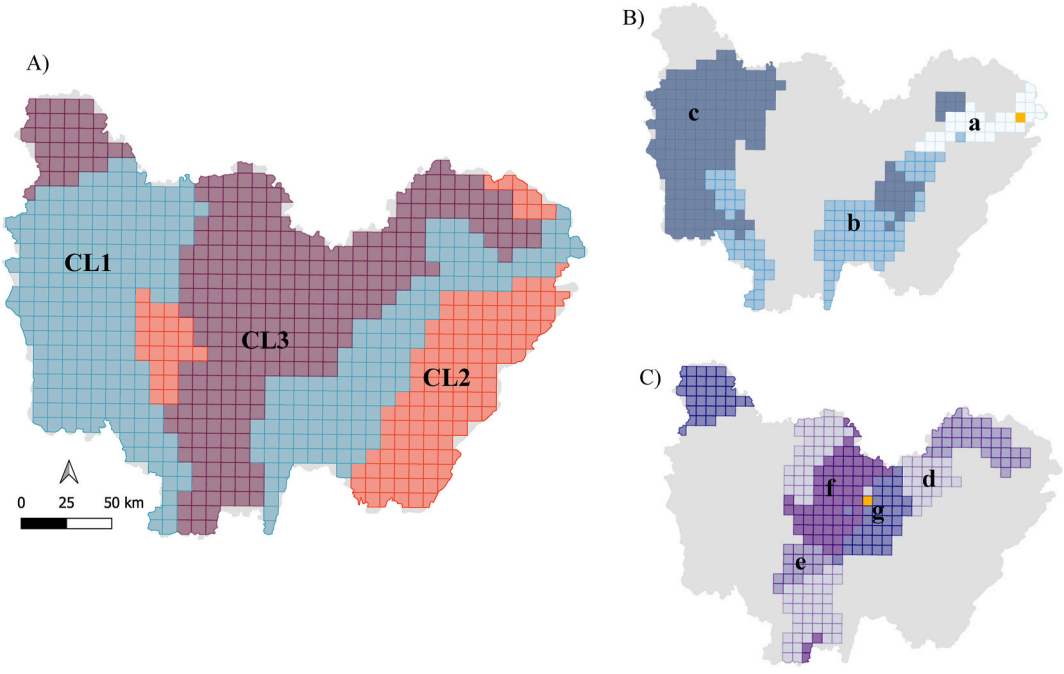

Fig. 6. Regional clustering based on meteorological variables (average temperature, relative humidity, wind and liquid precipitations) (A) and sub-clustering of areas of interest from SAFRAN: Montbéliard (B) and Dijon (C). The letters a, b and c correspond to sub-clusters of Montbéliard cluster. The letters d, e, f and g correspond to sub-clusters of Dijon cluster.

Cluster 1 – CL1 (in blue, Fig. 6A), called “relief marges”, includes the city of Montbéliard. It records an average wind speed of 2.75 m/s, the highest average temperature (6.57 °C) and a medium rainfall rate (2.4 mm/day).

Cluster 2 – CL2 (in red, Fig. 6A), called “relief areas” (Jura and Morvan) is defined by the highest rainfall rates (3.58 mm/day) and the lowest average temperature (4.34 °C) and relative humidity (82.8%).

Cluster 3 – CL3 (in purple, Fig. 6A), called “plateau - low altitudes” includes Dijon and records the highest relative humidity rates (84.6%) and the best ventilation (wind speed: 3.09 m/s).

While the temporal variability of the meteorological parameters studied follows the same patterns during the "particle season" (Fig. 7), as expected, here is a notable difference between low-altitude (CL3) and high-altitude clusters (CL1 and CL2). Indeed, the more elevated areas (CL1 and CL2) are also more exposed to the phenomenon of precipitation with the highest values in the case of mountains (up to 10 mm). Ventilation appears to be lower in areas such as the Jura massif or the Morvan, influenced by the topography and the potential barrier effect favouring the accumulation phenomenon.

Fig. 7 highlights relatively small difference between Cluster 1 (including Montbéliard) and Cluster 3 (including Dijon). To better understand the specific characteristics of the two cities, and to highlight the influence of topography and local environmental factors on air quality, we found it useful to create sub-clusters for Clusters 1 and 3. As shown in Fig. 6B, Montbéliard’s distinct characteristics are observable, particularly in terms of lower temperatures (6.35 °C compared to approximately 6.60 °C in other sub-clusters of CL1) and a relatively low average wind speed (2.83 m/s, the maximum of the CL3 sub-clusters). Dijon sub-clusters don’t show much variability whatever the meteorological variable targeted, but present the advantages of reflecting, at this fine spatial scale, the open/close characteristics of the areas.

When considering the average $PM_{2.5}$ concentrations, calculated using the IDW (Inverse Distance Weighting) interpolation method (Shepard, 1968), we observe that the Montbéliard sub-cluster exhibits an average concentration of 14.43 µg/m³, which is close to the daily WHO recommended value of 15 µg/m³. This is in stark contrast to the relatively consistent $PM_{2.5}$ levels across the Dijon sub-clusters, where the highest concentration recorded is only 11.96 µg/m³.

This difference confirms the climate-topographic effect on air quality during the particulate season in eastern France: Montbéliard’s valley setting fosters pollution accumulation while Dijon benefits from better natural ventilation due to its more open environment. Here, the creation of sub-clusters, which reflect the spatial opening and closing of areas at the kilometer scale, allows for a more granular analysis of pollution spatial distribution. This is particularly useful given the grid used for climate variables in our study, SAFRAN, which operates at an 8 km spatial resolution. This finer resolution of climate grids enables a more detailed understanding of spatial variability in PM at finer scale, compared to coarser scale products such as the CAMS (Copernicus Atmosphere Monitoring Service) dataset, which typically operates at much larger spatial scales (e.g., 50 km or more).

As a summary, the consideration of “opening” and “closing” of areas at the spatial scale of 8 km introduces a groundbreaking approach for air quality assessment. While CAMS provides valuable insights into larger-scale atmospheric conditions and pollutant distributions (Inness et al., 2019), its coarser resolution makes it less effective for capturing localized variations that can be critical in understanding particulate matter concentrations in specific urban settings. The finer spatial granularity of the SAFRAN grid, in contrast, offers an important intermediate scale that better aligns with the needs of urban air quality studies, enabling more accurate and localized assessments.

To follow, as the meteorological differences between the sub-clusters of Dijon and Montbéliard are not that marked, we complemented this analysis looking at the regional atmospheric circulation patterns in order to understand their influence on air masses and therefore on the pollutants present and their concentration. In the following, we adopt the GWL approach, which allows us to integrate a synoptic analysis beyond the principal meteorological variables (such as temperature, wind etc.). The use of GWL provides a more comprehensive view of atmospheric conditions by taking into account the structure of large-scale weather systems. The analysis focuses on two specific years: 2018 and 2020.

3.2.2. *Daily $PM_{2.5}$ levels influenced by atmospheric circulation*

A comparative study was carried out between 2018 and 2020 (Fig. 8a & b.), which are considered to be similar in terms of meteorology, based on Großwetterlagen (GWL). The objective was to classify types of weathers according to the presence of high- (in red, Fig. 8) or low-pressure (in blue, Fig. 8) systems and associate the concentration levels measured in Dijon and Montbéliard, particularly during the

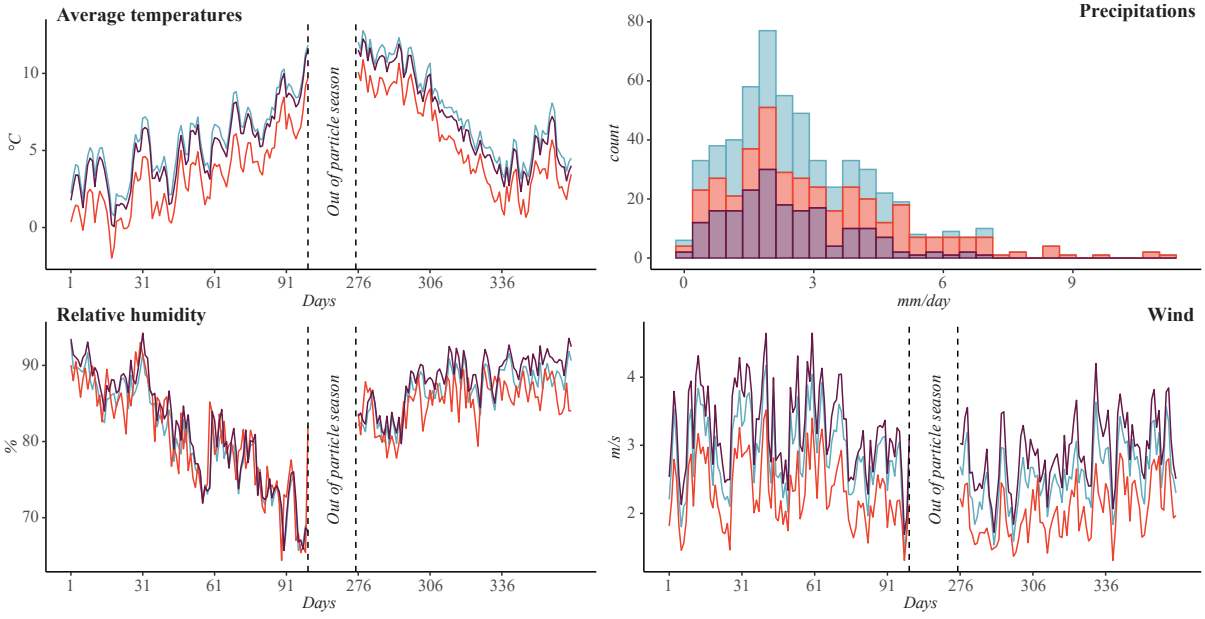

Fig. 7. Average values of temperature, relative humidity, liquid precipitations and wind speed during the particulate season for each cluster. Cluster 1 in blue, Cluster 2 in red and Cluster 3 in purple. Values are averaged over the 2015–2022 period.

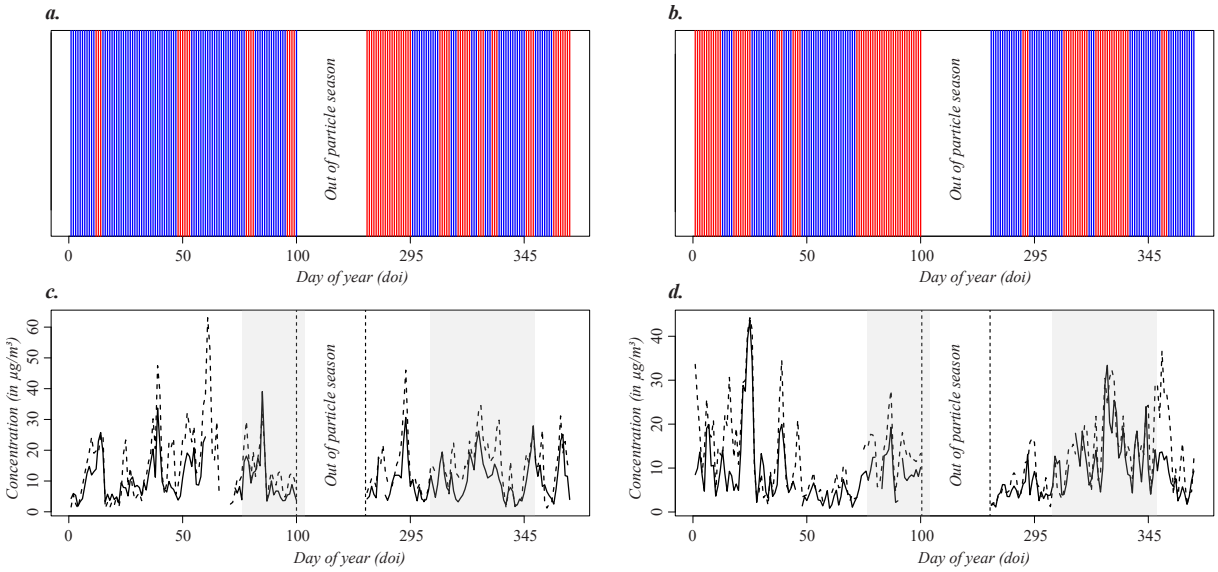

Fig. 8. Atmospheric conditions based on GWL: high-pressure (in red), low-pressure (in blue) for the years 2018 (a.) and 2020 (b.). $PM_{2.5}$ concentration levels measured in Montbéliard (in dotted line) and Dijon (in solid line) in 2018 (c.) and 2020 (d.) during the « particulate season». COVID-19 lockdowns are represented in light grey areas.

"particulate season". Both years present numerous alternations between high and low-pressure systems, especially during the second part of the particulate season (the end of October, November and December). The year 2018 starts with low pressure, accompanied by rather low $PM_{2.5}$ concentration levels (around 5 µg/m^3), followed by a February–March period that was mainly unsettled but with high $PM_{2.5}$ concentrations, with Montbéliard reaching its annual maximum of >60 µg/m^3 at the beginning of March. On the other hand, at the end of the year, there is a quick alternation of low-pressure and high-pressure weather, with $PM_{2.5}$ concentrations being higher during high-pressure systems, and concentration levels decreasing more or less rapidly once the low-pressure weather settles, depending on the duration of the preceding episode (e.g., Fig. 8). The year 2020 begins with high pressure, with episodes lasting several days, affecting concentration levels a few days later. This raises questions about the performance of the dispersion-accumulation phenomenon. The end of the year provides a good example, with Montbéliard seeing an increase in $PM_{2.5}$ levels around the 345th day (approx. +15 µg/m^3), raising questions about past high-pressure periods combined with a slower decrease in concentrations at this site compared to Dijon (approx. +3 µg/m^3).

Atmospheric blocking, which refers to a stable atmospheric process due to the formation of a warm, inactive anticyclone in the middle troposphere at mid and high latitudes, plays a key role in these phenomena (Xu et al., 2019). As known from the literature, high-pressure systems generally lead to stagnation and accumulation of pollutants, as the lack of atmospheric circulation traps the air near the ground, preventing the dispersion of particulate matter (Barmpadimos et al., 2011; Lyamani et al., 2012). However, what is interesting in this study is the observation of an inertia in the accumulation of pollution, particularly in areas with specific topographic features, such as Montbéliard. While the theory suggests that the air should clear once the high-pressure system breaks, we observe that in Montbéliard, the pollution persists for longer periods, likely due to the local topography acting as a "dispersion barrier" (J. Baldasano et al., 2003). This is obvious in Fig. 8, where the $PM_{2.5}$ concentrations show a delayed response to atmospheric changes, highlighting the important role that the local landscape plays in shaping the dynamics of air pollution accumulation.

To complete this study, the case of COVID-19 and the analysis of its lockdowns is a good opportunity to explore the impact of changes in pollution emission sources. Indeed, the pollution analysis during the COVID-19 lockdowns makes it possible to remove traffic from the other pollution sources (here mainly from heating-residential activities) to a greater or lesser extent and thus to discriminate its effects. We can therefore suggest that the effect should be more marked in Montbéliard (see diurnal cycle in Fig. 5b) than in Dijon (Fig. 5a).

3.3. *The case study of the $PM_{2.5}$ pollution during the COVID-19 lockdowns in 2020*

A comparative analysis of the first and second COVID-19 lockdowns in 2020 revealed several interesting findings regarding the joyplots of $PM_{2.5}$ concentrations in Dijon and Montbéliard (Fig. 9). During the first lockdown, which took place in spring, the concentration levels in Montbéliard were similar to those in 2018, while in Dijon, a noticeable decrease in $PM_{2.5}$ levels occurred from 9 µg/m^3 in 2018 to 6 µg/m^3 in 2020. This difference in response between the two cities could be attributed to the local environmental and meteorological conditions. In Montbéliard, despite the significant reduction in traffic, the expected improvement in air quality was not as pronounced because of the climate-topography effect described before (§3.1.2). In contrast, the $PM_{2.5}$ levels in Dijon showed a clearer decrease, likely linked to the open aspect of the area. It is noteworthy that for PM_{10} the reduction was not as pronounced in Dijon, notably due to the proximity of agricultural activities and the resuspension of particles, especially as the first lockdown took place during the agricultural season. This highlights the complex interplay between meteorological conditions, local emissions (e.g., road traffic and agricultural practices), and topography.

In contrast, the second lockdown (2020) exhibited a clearer and more contrasting effect. While Montbéliard, rather traffic, saw a slight decrease in $PM_{2.5}$ concentrations (from 17 µg/m^3 to 15 µg/m^3), Dijon experienced a surprising increase, from 7 µg/m^3 to 11 µg/m^3, in link with the residential heating. In addition, the weather conditions are favorable to accumulation, which means that the effect of PM pollution in Dijon is amplified. Both cities exhibited a wider range of values and higher median concentrations compared to the first lockdown. This suggests that, in addition to changes in traffic (less marked than the first lockdown), other factors were at play, potentially the heating-residential effect more pronounced in Dijon than in Montbéliard because of the site located in a residential urban area associated with the

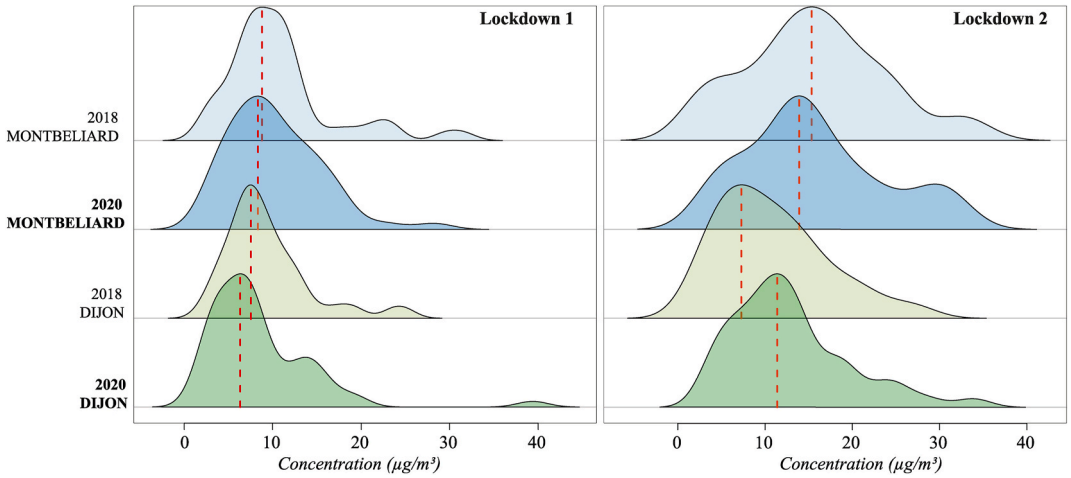

Fig. 9. Joyplot of daily $PM_{2.5}$ concentrations in Dijon (in green) and Montbéliard (in blue). Comparison of lockdowns periods in 2018 and 2020 (as a reminder: lockdown 1 from 17 March to 3 May 2020 and lockdown 2 from 30 October to 15 December 2020). The dashed red line indicates the main mode.

increase in tele-work. Moreover, the prolonged presence of high-pressure systems and thermal inversions during Lockdown 2 likely hindered the dispersion of pollutants, leading to their accumulation near the ground, notably in Dijon where the sources of pollution were more important than usual (in Fig. 8). Notably, these atmospheric conditions likely had a more significant impact on $PM_{2.5}$ concentrations than the reduction in traffic alone, reflecting the nuanced and context-dependent nature of air quality during the COVID-19 lockdowns.

The results from both lockdowns underscore the complexity of interpreting air quality data in times of reduced human activity. The diurnal cycles in both cities in 2018 and 2020 (Fig. 10) complete the previous analyzes. For instance, in Montbéliard, despite the decline in

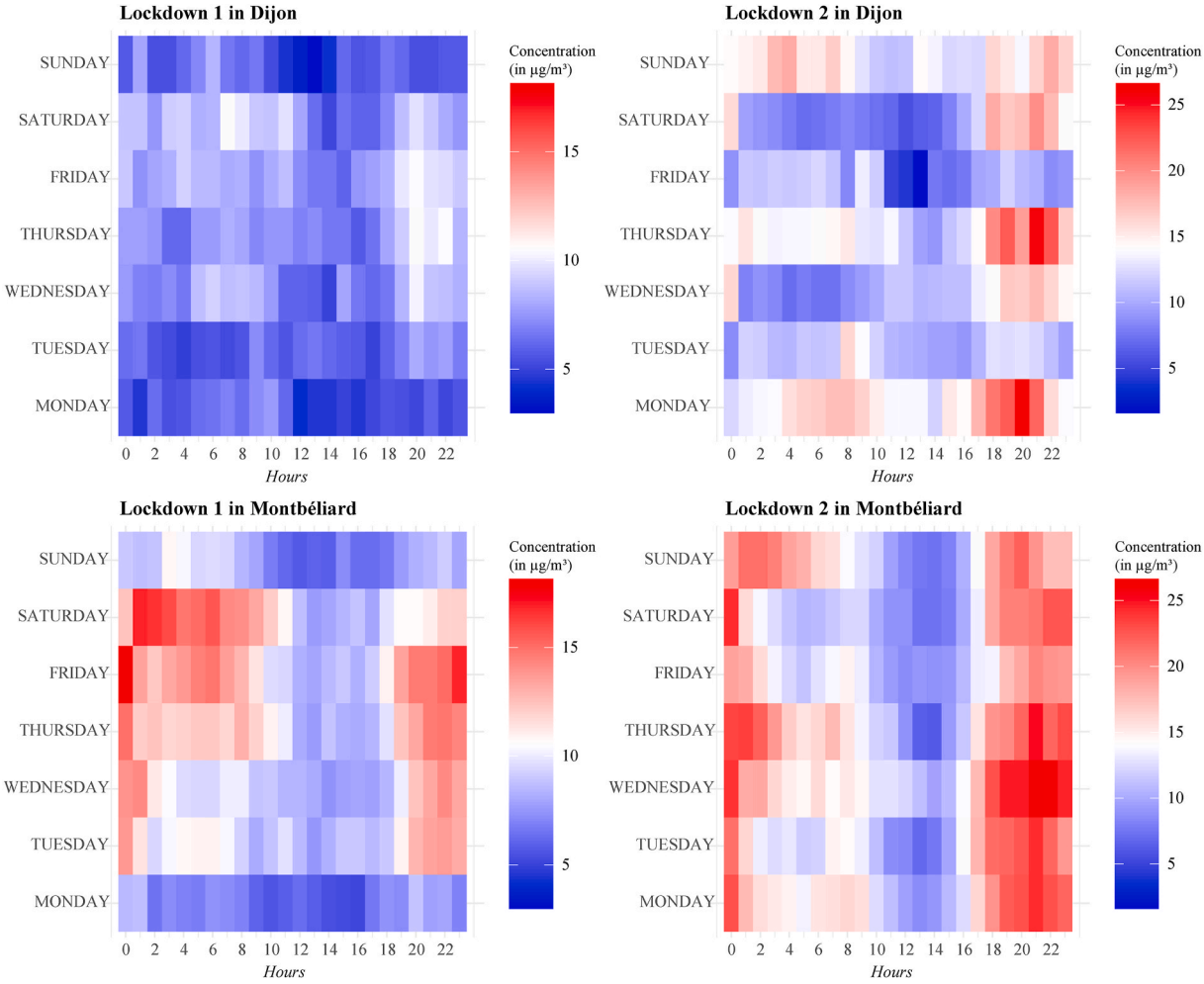

Fig. 10. Mean diurnal cycle of $PM_{2.5}$ concentrations during lockdowns 1 (column 1) and 2 (column 2) in 2020 in Dijon (line 1) and Montbéliard (line 2).

road traffic, the high concentration levels persisted and even showed a nocturnal cumulative effect during both lockdowns. This "recharging" of particulate matter on Monday nights, followed by a slight decrease over the weekend, suggests that residential heating and localized sources were still contributing significantly to pollution levels.

While some studies have observed a sharp decrease in NO_x levels during the COVID-19 lockdowns (J. M. Baldasano, 2020), the response of $PM_{2.5}$ concentrations is more ambiguous and depends heavily on local source emissions notably from residential heating, or meteorological conditions, and climate-topographic influences.

Looking ahead, the comparison of these two distinct phases of the COVID-19 pandemic provides valuable insights into the dynamics of particulate pollution. In the future, a comparison with post-pandemic conditions in 2024, when normal traffic and emissions have resumed, will be crucial to assess whether Montbéliard's specific characteristics such as its topography and traffic-related emission continue to drive elevated pollution levels, or if the return to normal conditions leads to significant changes in $PM_{2.5}$ concentrations. This will help in further discrediting or confirming the role of various pollution sources and will contribute to our understanding of the long-term impact of lockdown-induced behaviour changes on air quality.

4. Conclusion

This study on air quality in eastern France examines PM pollution, focusing on regions with generally good air quality, but with concerns about the 2021 WHO $PM_{2.5}$ guidelines. A clear seasonal pattern of $PM_{2.5}$ pollution is observed in both Dijon and Montbéliard, driven by an apparent climate-topography effect. The "particulate season," from October to April, shows average concentrations of 11.55 $\mu g/m^3$ in Dijon and 15 $\mu g/m^3$ in Montbéliard. Moreover, daily $PM_{2.5}$ concentrations are highly influenced by alternating high- and low-pressure systems.

The method developed in this study, which establishes a link between weather patterns and air quality through the analysis of geographically close but contrasting sites, paves the way for the generalization of this approach to other cities, particularly in Europe. What is innovative here is the adoption of an integrated approach that allows the joint analysis of air quality in relation to several factors such as temperature, topography, and wind something that is generally not done in traditional studies. Indeed, conventional approaches often focus on one factor at a time (e.g., air quality vs. temperature, air quality vs. topography, air quality vs. wind) but do not consider these factors into a combined analysis. This comparative approach, based on both quantitative (SAFRAN) and qualitative (GWL) weather types, enables a more nuanced understanding of local dynamics and opens up perspectives for a more comprehensive analysis of air quality.

The study also explores the effect of COVID-19 lockdowns on $PM_{2.5}$ levels. The effects are very contrasted in the two cities studied. In Montbéliard (under intermediate traffic influence) air quality remains relatively unchanged whatever the lockdowns because of the dominating climate-topography effects. In Dijon (under residential influence), air quality improves slightly during the first lockdown (due to a clear traffic decrease), but worsens during the second lockdown as heating-residential increases related to tele-work. These findings show that reducing traffic alone does not ensure compliance with WHO $PM_{2.5}$ limits, as PM pollutant is multi-sources and complex.

Furthermore, even during the COVID-19 periods, fine particulate concentrations showed an alarming proximity to annual chronic disease thresholds, highlighting the persistence of daily exposure to potentially harmful pollution levels. This reinforces the public health challenge and demonstrates that, even under exceptional conditions, air quality management remains crucial. In particular by looking at each pollutant individually. These results support the idea that this method could be transferable to other regions, emphasizing the long-term importance of air pollution monitoring for public health.

CRediT authorship contribution statement

Sarah Marion: Writing – original draft, Methodology, Investigation, Formal analysis. **Nadège Martiny:** Writing – review & editing, Supervision, Resources, Project administration. **Suzanne Crumeyrolle:** Writing – review & editing. **Olivier Planchon:** Writing – review & editing, Resources. **Anaïs Detournay:** Resources.

Funding

This research did not receive any specific funding from public, commercial or not-for-profit funding bodies.

Declaration of competing interest

The authors declare that they have no known competing financial interests or personal relationships that could have appeared to influence the work reported in this paper.

Acknowledgments

We would like to acknowledge Pablo Campargue from ATMO Bourgogne Franche – Comté for the data collection access and his listening and advices.

References

Arkouli, M., Ulke, A.G., Endlicher, W., Baumbach, G., Schultz, E., Vogt, U., Müller, M., Dawidowski, L., Faggi, A., Wolf-Benning, U., Scheffknecht, G., 2010. Distribution and temporal behavior of particulate matter over the urban area of Buenos Aires. Atmos. Pollut. Res. 1 (1), 1–8. https://doi.org/10.5094/APR.2010.001.

Badach, J., Wojnowski, W., Gębicki, J., 2023. Spatial aspects of urban air quality management : estimating the impact of micro-scale urban form on pollution dispersion. Comput. Environ. Urban Syst. 99, 101890. https://doi.org/10.1016/j.compenvurbsys.2022.101890.

Baldasano, J.M., 2020. COVID-19 lockdown effects on air quality by NO_2 in the cities of Barcelona and Madrid (Spain). Sci. Total Environ. 741, 140353. https://doi.org/10.1016/j.scitotenv.2020.140353.

Baldasano, J., Valera, E., Jimenez, P., 2003. Air quality data from large cities. Sci. Total Environ. 307 (1–3), 141–165. https://doi.org/10.1016/S0048-9697(02)00537-5.

Bárdossy, A., Caspary, H.J., 1990. Detection of climate change in Europe by analyzing European atmospheric circulation patterns from 1881 to 1989. Theor. Appl. Climatol. 42 (3), 155–167. https://doi.org/10.1007/BF00866871.

Barmpadimos, I., Hueglin, C., Keller, J., Henne, S., Prévôt, A.S.H., 2011. Influence of meteorology on PM_{10} trends and variability in Switzerland from 1991 to 2008. Atmos. Chem. Phys. 11 (4), 1813–1835. https://doi.org/10.5194/acp-11-1813-2011.

Bernard, J., Bocher, E., Gousseff, M., Leconte, F., Wiederhold, E.L.S., 2024. A generic algorithm to automatically classify urban fabric according to the Local Climate Zone system : implementation in GeoClimate 0.0.1 and application to French cities. Geosci. Model Dev. (GMD) 17 (5), 2077. https://doi.org/10.5194/gmd-17-2077-2024.

Bocher, E., Bernard, J., Wiederhold, E., Leconte, F., Petit, G., Palominos, S., Noûs, C., 2021. GeoClimate : a Geospatial processing toolbox for environmental and climate studies. J. Open Source Softw. 6 (65), 3541. https://doi.org/10.21105/joss.03541.

Brunekreef, B., Strak, M., Chen, J., Andersen, Z.J., Atkinson, R., Bauwelinck, M., Bellander, T., Boutron, M.-C., Brandt, J., Carey, I., Cesaroni, G., Forastiere, F., Fecht, D., Gulliver, J., Hertel, O., Hoffmann, B., de Hoogh, K., Houthuijs, D., Hvidtfeldt, U., et al., 2021. Mortality and Morbidity Effects of Long-Term Exposure to Low-Level $PM_{2.5}$, BC, NO_2, and O_3 : an Analysis of European Cohorts in the ELAPSE Project. Research Reports: Health Effects Institute, 2021, p. 208.

Cantat, O., Savouret, E., 2014. A catalog of 'weather types' in metropolitan France. Climatologie 11, 65–71. https://doi.org/10.4267/climatologie.584.

Cesari, D., De Benedetto, G.E., Bonasoni, P., Busetto, M., Dinoi, A., Merico, E., Chirizzi, D., Cristofanelli, P., Donateo, A., Grasso, F.M., Marinoni, A., Pennetta, A., Contini, D., 2018. Seasonal variability of $PM_{2.5}$ and PM_{10} composition and sources in an urban background site in Southern Italy. Sci. Total Environ. 612, 202–213. https://doi.org/10.1016/j.scitotenv.2017.08.230.

Chen, J., Hoek, G., 2020. Long-term exposure to PM and all-cause and cause-specific mortality : a systematic review and meta-analysis. Environ. Int. 143, 105974. https://doi.org/10.1016/j.envint.2020.105974.

Chen, Z., Xie, X., Cai, J., Chen, D., Gao, B., He, B., Cheng, N., Xu, B., 2018. Understanding meteorological influences on PM concentrations across China : a temporal and spatial perspective. Atmos. Chem. Phys. 18 (8), 5343–5358. https://doi.org/10.5194/acp-18-5343-2018.

Cheng, B., Ma, Y., Zhao, Y., Qin, P., Feng, F., Liu, Z., Wang, W., Zhang, Y., 2024. Influence of topography and synoptic weather patterns on air quality in a valley

basin city of Northwest China. Sci. Total Environ. 934, 173362. https://doi.org/10.1016/j.scitotenv.2024.173362.
Dominici, F., Schwartz, J., Di, Q., Braun, D., Choirat, C., Zanobetti, A., 2019. Assessing Adverse Health Effects of Long-Term Exposure to Low Levels of Ambient Air Pollution : Phase 1, vol. 2019. Research Reports: Health Effects Institute, p. 200.
Dupont, J., Haeffelin, M., Badosa, J., Elias, T., Favez, O., Petit, J., Meleux, F., Sciare, J., Crenn, V., Bonne, J.L., 2016. Role of the boundary layer dynamics effects on an extreme air pollution event in Paris. Atmos. Environ. 141 (2), 571–579. https://doi.org/10.1016/j.atmosenv.2016.06.061.
Giovannini, L., Ferrero, E., Karl, T., Rotach, M., Staquet, C., Trini Castelli, S., Zardi, D., 2020. Atmospheric pollutant dispersion over complex Terrain : challenges and needs for improving air quality measurements and modeling. Atmosphere 11, 646. https://doi.org/10.3390/atmos11060646.
Health Effects Institute & Institute for Health Metrics, 2020. *State Of Global Air 2020* [Special Report]. Health Effects Institute.
Hess, N.P., Brezowsky, H., 1952. Katalog der Großwetterlagen Europas, 39 S. 7, Beil.
IARC, 2015. Outdoor Air Pollution, vol. 109. https://publications.iarc.fr/Book-And-Report-Series/Iarc-Monographs-On-The-Identification-Of-Carcinogenic-Hazards-To-Humans/Outdoor-Air-Pollution-2015.
Inness, A., Ades, M., Agustí-Panareda, A., Barré, J., Benedictow, A., Blechschmidt, A.-M., Dominguez, J.J., Engelen, R., Eskes, H., Flemming, J., Huijnen, V., Jones, L., Kipling, Z., Massart, S., Parrington, M., Peuch, V.-H., Razinger, M., Remy, S., Schulz, M., Suttie, M., 2019. The CAMS reanalysis of atmospheric composition. Atmos. Chem. Phys. 19 (6), 3515–3556. https://doi.org/10.5194/acp-19-3515-2019.
Klaus, D., 1993. Zirkulations- und Persistenzänderungen des europäischen Wettergeschehens im Spiegel der Grosswetterlagenstatistik (Changes in the Circulation and Persistence of European Weather Types as Reflected in the Statistics of Large-Scale Weather Situations). Erdkunde 47 (2), 85–104.
Köppen, W., 1936. Das geographische System der Klimate: Vol. Band 1, Teil C. Gebrüdcr Borntraeger.
Kukkonen, J., Pohjola, M., S Sokhi, R., Luhana, L., Kitwiroon, N., Fragkou, L., Rantamäki, M., Berge, E., Ødegaard, V., Håvard Slørdal, L., Denby, B., Finardi, S., 2005. Analysis and evaluation of selected local-scale PM_{10} air pollution episodes in four European cities : Helsinki, London, Milan and Oslo. Atmos. Environ. 39 (15), 2759–2773. https://doi.org/10.1016/j.atmosenv.2004.09.090.
Le Moigne, P., Besson, F., Martin, E., Boé, J., Boone, A., Decharme, B., Etchevers, P., Faroux, S., Habets, F., Lafaysse, M., Leroux, D., Rousset-Regimbeau, F., 2020. The latest improvements with SURFEX v8.0 of the Safran–Isba–Modcou hydrometeorological model for France. Geosci. Model Dev. (GMD) 13 (9), 3925–3946. https://doi.org/10.5194/gmd-13-3925-2020.
Loones, F., Rossignol, P., Darouache, N.E., François, S., 2021. Un quart des habitants régulièrement exposé aux particules fines $PM_{2.5}$ (89), 4. https://www.insee.fr/fr/statistiques/5435110.
Lupo, A.R., Oglesby, R.J., Mokhov, I.I., 1997. Climatological features of blocking anticyclones : a study of Northern Hemisphere CCM1 model blocking events in present-day and double CO_2 concentration atmospheres. Clim. Dynam. 13, 181–195. https://doi.org/10.1007/s003820050159.
Lyamani, H., Fernández-Gálvez, J., Pérez-Ramírez, D., Valenzuela, A., Antón, M., Alados, I., Titos, G., Olmo, F.J., Alados-Arboledas, L., 2012. Aerosol properties over two urban sites in South Spain during an extended stagnation episode in winter season. Atmos. Environ. 62, 424–432. https://doi.org/10.1016/j.atmosenv.2012.08.050.
Met One Instruments, 2024. BAM 1020 beta attenuation mass monitor. https://metone.com/wp-content/uploads/2024/01/BAM-1020-O-v1.2-20240129.pdf.
Météo France, 2021. Bilan climatique de l'année 2020 sur la France métropolitaine. https://meteofrance.fr/sites/meteofrance.fr/files/files/editorial/Bilan_annuel_2020_d%C3%A9finitif_140121.pdf.
Mokhov, I.I., Timazhev, A.V., Lupo, A.R., 2014. Changes in atmospheric blocking characteristics within Euro-Atlantic region and Northern Hemisphere as a whole in the 21st century from model simulations using RCP anthropogenic scenarios. Global Planet. Change 122, 265–270. https://doi.org/10.1016/j.gloplacha.2014.09.004.
Planchon, O., Quénol, H., Dupont, N., Corgne, S., 2009. Application of the Hess-Brezowsky classification to the identification of weather patterns causing heavy winter rainfall in Brittany (France). Nat. Hazards Earth Syst. Sci. 9 (4), 1161–1173. https://doi.org/10.5194/nhess-9-1161-2009.
Planchon, O., Quénol, H., Irimia, L., Patriche, C., 2015. European cold wave during February 2012 and impacts in wine growing regions of Moldavia (Romania). Theor. Appl. Climatol. 120 (3), 469–478. https://doi.org/10.1007/s00704-014-1191-2.
Pope, C., Burnett, R., Thun, M., Calle, E., Krewski, D., Ito, K., Thurston, G., 2002. Lung cancer, cardiopulmonary mortality, and long-term exposure to fine particulate air pollution. JAMA, J. Am. Med. Assoc. 287, 1132–1141. https://doi.org/10.1001/jama.287.9.1132.
Quénol, H., Planchon, O., Wahl, L., 2008. Méthodes d'identification des climats viticoles. Bulletin de la Société Géographique de Liège. https://popups.uliege.be/0770-7576/index.php?id=1553.
Samek, L., Turek-Fijak, A., Skiba, A., Furman, P., Styszko, K., Furman, L., Stegowski, Z., 2020. Complex characterization of fine fraction and source contribution to $PM_{2.5}$ mass at an urban area in central europe. Atmosphere 11 (10). https://doi.org/10.3390/atmos11101085. Article 10.
Santé Publique France, 2021. Impact of ambient air pollution on mortality in metropolitan France : reduction related to Spring 2020 lockdown and new data for total burden of impact for the period 2016-2019, 12. https://www.santepubliquefrance.fr/presse/2021/pollution-de-l-air-ambiant-nouvelles-estimations-de-son-impact-sur-la-sante-des-francais.
Shepard, D., 1968. A two-dimensional interpolation function for irregularly-spaced data. In: Proceedings of the 1968 23rd ACM National Conference on, pp. 517–524. https://doi.org/10.1145/800186.810616.
Shukla, K., Aggarwal, S.G., 2022. A technical overview on beta-attenuation method for the monitoring of particulate matter in ambient air. Aerosol Air Qual. Res. 22 (12), 220195. https://doi.org/10.4209/aaqr.220195.
Soubeyroux, J.-M., Martin, E., Franchisteguy, L., Habets, F., Noilhan, J., Baillon, M., Regimbeau, F., Vidal, J.-P., Lemoigne, P., Morel, S., 2008. Safran-Isba-Modcou (SIM) : Un outil pour le suivi hydrométéorologique opérationnel et les études. Meteorol. 8 (63), 40. https://doi.org/10.4267/2042/21890.
Stewart, I.D., Oke, T.R., 2012. Local climate Zones for urban temperature studies. Bull. Am. Meteorol. Soc. 93 (12), 1879–1900. https://doi.org/10.1175/BAMS-D-11-00019.1.
Xu, T., Song, Y., Liu, M., Cai, X., Zhang, H., Guo, J., Zhu, T., 2019. Temperature inversions in severe polluted days derived from radiosonde data in North China from 2011 to 2016. Sci. Total Environ. 647, 1011–1020. https://doi.org/10.1016/j.scitotenv.2018.08.088.
Zhang, J., Chen, J., Zhu, W., Ren, Y., Cui, J., Jin, X., 2024. Impact of urban space on $PM_{2.5}$ distribution : a multiscale and seasonal study in the Yangtze River Delta urban agglomeration. J. Environ. Manag. 363, 121287. https://doi.org/10.1016/j.jenvman.2024.121287.
Zhang, L., An, J., Liu, M., Li, Z., Liu, Y., Tao, L., Liu, X., Zhang, F., Zheng, D., Gao, Q., Guo, X., Luo, Y., 2020. Spatiotemporal variations and influencing factors of $PM_{2.5}$ concentrations in Beijing, China. Environmental Pollution 262, 114276. https://doi.org/10.1016/j.envpol.2020.114276.